

# Fluorescence Resonance Energy Transfer from Sulfonated Graphene to Riboflavin: A Simple Way to Detect Vitamin B<sub>2</sub>

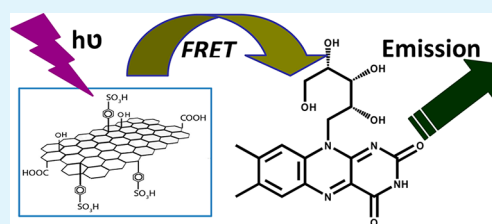
Aniruddha Kundu, Sudipta Nandi, Rama K. Layek, and Arun K. Nandi\*

Polymer Science Unit, Indian Association for the Cultivation of Science, Jadavpur, Kolkata-700 032, India

## S Supporting Information

**ABSTRACT:** We have prepared sulfonated graphene (SG) by diazonium coupling technique and it has been characterized by UV–vis absorption spectroscopy, Raman spectroscopy, electron microscopy, energy-dispersive spectroscopy (EDS), EDS elemental mapping, X-ray photoelectron spectroscopy (XPS), and FTIR spectroscopy. The photoluminescence (PL) property of SG at different pH (pH 4, 7, and 9.2) has been investigated and SG shows highest PL-intensity and quantum yield at pH 4 compared to those at higher pH and that of GO at pH 4. Due to the strong overlap between the emission spectrum of SG and absorption spectrum of riboflavin (RF, vitamin B<sub>2</sub>) at pH 4, it has been tactfully used as donor for the fluorescence resonance energy transfer (FRET) process. However, graphene oxide (GO) does not exhibit any FRET with RF at an identical condition due to its much lower quantum yield. We have demonstrated a selective detection of vitamin B<sub>2</sub> in presence of nucleic acid (DNA, RNA), protein (BSA), amino acid (Lysine) and other water-soluble vitamins (Becosules, Zevit capsules) based on the spontaneous FRET from PL-active SG (donor) to RF (acceptor). The calibration curve indicates excellent affirmation to detect vitamin B<sub>2</sub> using FRET and it is superior to the ordinary fluorescence method of detecting RF in presence of different biomolecules.

**KEYWORDS:** sulfonated graphene, TEM, fluorescence, riboflavin, Raman spectra, Förster distance



## INTRODUCTION

Resonance energy transfer (RET) is a nonradiative photo-physical process that occurs between a donor and an acceptor, the donor at an excited state transfer energy to the acceptor present at the ground state through long-range dipole–dipole interactions.<sup>1</sup> It is broadly classified as fluorescence resonance energy transfer (FRET),<sup>2</sup> bioluminescence resonance energy transfer (BRET),<sup>3</sup> and chemiluminescence resonance energy transfer (CRET).<sup>4</sup> FRET occurs by an intermolecular energy transfer mechanism where the energy absorbed by a fluorescent molecule (donor) is transferred nonradiatively to the acceptor molecule. This is experimentally manifested by a simultaneous quenching of the donor fluorescence and an electronic excitation of the acceptor molecule suggesting the transfer of energy without the appearance of a photon due to the long-range dipole–dipole interactions between the donor and acceptor.<sup>5</sup> The FRET efficiency is highly sensitive to many factors, such as quantum yield of donor, the spectral overlap between emission bands of fluorescent donor and absorption bands of the acceptor and the relative dipole orientation of the two, thus the spatial distance between the two emerges as an influential factor.<sup>2,5</sup> These characteristic features of FRET principles promote its versatile application in diverse fields, e.g., to study the conformational distribution and dynamics of biological molecules such as DNA,<sup>6,7</sup> protein,<sup>8,9</sup> etc., polymer molecules and in analytical science to construct variety of sensing and diagnostic platforms.<sup>10–12</sup> Recently, Chen et al. have reported FRET detection of label free target DNA in a

PDMS microfluidic channel using two fluorescently labeled nucleic acid probes.<sup>13</sup>

Riboflavin (RF), commonly called vitamin B<sub>2</sub>, is an important biological molecule because it is one of the most widely distributed water-soluble vitamins and is easily absorbed micronutrient that becomes actively absorbed into eukaryotic cells.<sup>14</sup> The majority of riboflavin is converted to its cofactor forms, flavin mononucleotide (FMN) and flavin adenine dinucleotide (FAD); therefore, it is required by all flavoproteins.<sup>15,16</sup> Vitamin B<sub>2</sub> is also required for a wide variety of cellular processes, such as metabolism of fats, ketone bodies, carbohydrates, and proteins, thus plays a key role in the human diet. Earlier methods used for the determination of RF such as high performance liquid chromatography (HPLC),<sup>17,18</sup> capillary electrophoresis<sup>19,20</sup> suffer a multiple shortcomings, including the delayed response, lack of selectivity, and the above processes also require large amount of costly solvents. Comparing with the above techniques, the fluorescent method is a versatile analytical tool since it has many advantages, including greater simplicity, broader applicability, and higher sensitivity. In contrast to the high sensitivity of fluorescence, but being quenched because of the presence of different components in the biological systems, FRET has been recognized as an exceptionally sensitive method that promises an extensive opportunity for bioanalytical applications.

Received: May 8, 2013

Accepted: July 9, 2013

Published: July 9, 2013

Graphene, along with its counterpart, graphene oxide (GO), is a two-dimensional (2D) monatomic carbon material that has recently attracted persistent interest to the scientific community because of its remarkable opto-electronic, mechanical and thermal properties.<sup>21,22</sup> Because of its unique characteristics such as high water dispersibility,<sup>23</sup> large surface area, facile surface modification,<sup>24–26</sup> and strong photoluminescence,<sup>27</sup> GO has been used to design a variety of fluorescent biosensor with enhanced performance.<sup>28–35</sup> The photoluminescence (PL) property of GO may originate from the recombination of electron–hole pairs generated within the localized graphitic  $sp^2$  states arising from the various defect structure produced from the harsh oxidation of graphite to GO, although different propositions are also forwarded in the recent reports.<sup>36–40</sup> Further, the pH-dependent PL property of GO has been recently revealed,<sup>41–43</sup> producing a new pathway to develop different sensors.<sup>44–46</sup> The color quenching capacity of GO has also been used to detect heparin on the basis of label-free colorimetric strategy.<sup>47</sup>

In this article, we report the pH dependent PL property of sulfonated graphene (SG), to the best of our knowledge for the first time. Recently, SG has been used for various applications<sup>48–50</sup> and herein, we have developed a simple platform to detect vitamin-B<sub>2</sub> using the spontaneous FRET from SG to vitamin B<sub>2</sub> in presence of the other water-soluble vitamins, nucleic acids (DNA, RNA), protein (bovine serum albumin, BSA), blood serum, and amino acid (Lysine) at pH 4. SG has been used because the as prepared aqueous dispersions of SG nanosheets are electrostatically stabilized in water due to the presence of sulfonic acid moieties favoring H-bond formation with water molecules and it also cause mutual repulsion from the other SG sheets.<sup>51</sup> These sulfonic acid groups accounts to the excellent solubility of SG over GO, with their presence alone being sufficient to produce a stable aqueous solution after chemical reduction of epoxy and hydroxyl groups from the basal plane.<sup>52</sup> In our earlier reports, we have used SG both as an ion-exchange platform and as a fluorescence quencher to sense DNA among the other biomolecules using the fluorescence property of ethidium bromide, a fluorescent dye.<sup>50</sup> But here the sensing property has been studied using only the fluorescence property of SG itself at a lower pH (pH 4) where its quantum yield is significantly higher than that of GO facilitating the FRET process to the vitamin B<sub>2</sub>.

## ■ EXPERIMENTAL SECTION

**Sample.** Graphite powder, sodium nitrite, sodium borohydride, sulfanilic acid, riboflavin, Calf thymus DNA (Type 1; sodium salt), RNA (diethyl amino ethanol salt, type IX from Torula Yeast), Bovine serum albumin (BSA), Flavin mononucleotide (FMN) were purchased from Sigma Aldrich (USA). Sodium nitrate, potassium permanganate, 35% hydrochloric acid (G.R. grade), hydrazine hydrate solution (99%, synthetic grade) were purchased from E- Merck (Mumbai), where as Becosules (Pfizer Limited, Mumbai, India); and Zevit (Glaxo Smith Kline, Mumbai, India) were purchased from Frank Ross pharmacy (Kolkata). All the reagents were used as received.

**Synthesis of Sulfonated Graphene from Graphene Oxide.** At first graphene oxide (GO) was prepared from the graphite powder by oxidizing with  $KMnO_4/NaNO_3$  mixture in concentrated  $H_2SO_4$  medium using Hummers method.<sup>53</sup> Sulfonated graphene (SG) was prepared from GO through aryl diazonium reaction of sulfanilic acid.<sup>51</sup> As prepared GO ( $1.0\text{ mg mL}^{-1}$ ) was sonicated for 1 h in an ultrasonic bath (60W, frequency 28 kHz, Model AVIOC, Eyela) until a clear brownish dispersion of GO had appeared. The syntheses of SG from GO comprises of three steps: (1) prereduction of GO with sodium

borohydride; (2) sulfonation with the aryl diazonium salt of sulfanilic acid; and (3) postreduction with hydrazine to remove oxygen functionality. At first 600 mg sodium borohydride solution in 15 mL of water was added into 75 mL of the exfoliated GO dispersion and its pH was adjusted at 9–10 by the addition of 5 wt % sodium carbonate solution. The mixture was then kept at 80 °C for 1 h under constant stirring followed by centrifuging and washing with double distilled water several times until the solution became neutral and it was redispersed in 75 mL of water for diazonium coupling. For this purpose, 52 mg of sulfanilic acid and 26 mg of sodium nitrite were dissolved in 10 mL of water with the addition of 0.5 mL of 1 M HCl at ice cooled condition and was kept for 2 h with stirring. It was centrifuged and washed repeatedly with water until it became neutral. The product was then redispersed in 100 mL of water and it was reduced with 2 mL of hydrazine hydrate solution under refluxed condition for 24 h at 100 °C. Finally, it was washed with water thoroughly and dried in vacuum at 60 °C.

**Preparation of Sample.** The SG was dispersed in acidic medium at pH 4 using buffer capsule and it was sonicated for half an hour, using an ultrasonic bath (60W, frequency 28 kHz, Model AVIOC, Eyela) to make a constant composition (0.004% w/v). DNA, RNA, BSA, Lysine solutions (0.02% w/v) were prepared by dissolving the required amount in acidic medium (pH 4). The concentration of DNA, RNA, BSA and Lysine were 0.04 mg/mL. In the case of blood serum, 50  $\mu\text{L}$  of serum was diluted to 500  $\mu\text{L}$  with water and it was then added to the SG solution. The volume of SG was kept constant while RF was varied during the fluorescence spectroscopic measurements. For determination of RF from the vitamin capsules, the capsules were first dissolved in 50 mL of buffer solution of pH 4 and it was then added to the SG solution gradually from 0 to 500  $\mu\text{L}$  to investigate the FRET phenomenon.

**Characterization. Microscopy.** The GO and SG dispersions were characterized by transmission electron microscopy (TEM JEOL, 2010EX) fitted with a CCD camera at an acceleration voltage of 200 kV. The samples were prepared by spreading a small drop of diluted GO and SG solution on carbon-coated copper grid, allowed to dry in air and finally in vacuum at 30 °C for about 3 days. The energy-dispersive spectroscopy (EDS), EDS elemental mapping experiments were performed from the TEM micrograph in the same instrument.

**Elemental Analysis.** Elemental analysis of SG was conducted using 2400 Series II CHNS Analyzer (Perkin-Elmer, USA).

**Spectroscopy.** The UV–vis absorption spectra of aqueous solutions of the samples (GO, SG, RF) at pH 4, were recorded with a UV–vis spectrophotometer (Hewlett-Packard, model 8453) using a cuvette of 1 cm path length.

Photoluminescence (PL) study was performed in a sealed cuvette and the emission was studied in a Horiba Jobin Yvon Fluoromax 3 instrument. Each sample in a quartz cell of 1 cm path length was excited at 320 nm wavelength and the emission scans were recorded from 350 to 610 nm using a slit width of 2 nm for both the excitation and emission with an increment of 1 nm wavelength having an integration time of 0.1 s.

FT-IR spectrum of SG was obtained from its thin film cast from the solutions on a silicon wafer using a Perkin-Elmer FT-IR instrument (spectrum100).

Raman spectra of reduced graphene oxide (RGO), SG at different pH were recorded using a micro-Raman spectrometer (Agitron). The sample solutions were taken in a quartz cell of 1 cm path length and were excited using 785 nm laser.

The X-ray photoelectron spectroscopic (XPS) study of SG and SG nanocomposite system was performed using a focused monochromatized Mg  $K\alpha$  X-ray source (1253.6 eV) in the XPS instrument (Omicron NanoTechnology 0571).

**Photoluminescence Quantum Yield Measurements.** The relative PL quantum yields (QY) of GO and SG were measured using quinine sulfate in 0.1 M  $H_2SO_4$  (quantum yield 0.55 at 320 nm) as a standard for the fluorescence quantum yield measurement. The values were calculated using the standard reference sample that has a fixed and known fluorescence quantum yield value according to the following equation<sup>5</sup>

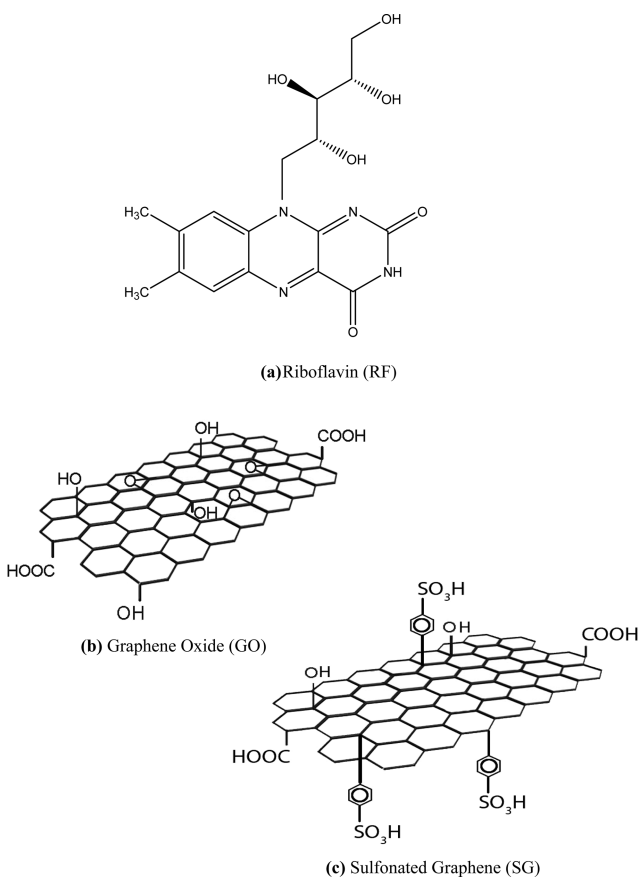
$$QY_{\text{sample}} = QY_{\text{std.}} \left[ \frac{(I/A)_{\text{sample}} \alpha (A/I)_{\text{std.}}}{(I/A)_{\text{std.}} \alpha (A/I)_{\text{sample}}} \right] \left( \frac{\eta^2_{\text{sample}}}{\eta^2_{\text{std.}}} \right) \quad (1)$$

where  $A$  is absorbance at the excitation wavelength,  $\eta$  is the refractive index and  $I$  is the integrated emission intensity calculated from the area under the emission peak on the same wavelength scale.

## RESULTS AND DISCUSSION

Scheme 1 presents the structures of riboflavin (RF), GO, and SG. The exfoliated nature of SG (Figure.1a) and GO (Figure

**Scheme 1. Structure of Riboflavin (RF), Graphene Oxide (GO), and Sulfonated Graphene (SG)**



S1 in the Supporting Information) sheets in aqueous medium at pH 4 has been characterized from the respective TEM images. The presence of different elements in SG (Figure.1b-d) and GO (see Figure S1a–c in the Supporting Information) are evaluated by energy dispersive X-ray spectroscopy (EDS) mapping. The corresponding EDS spectrum of SG has also been shown in Figure 1e, which clearly indicates the presence of sulfur in SG. The elemental analysis also confirms the presence of sulfur in SG and the amount of sulfur is found to be 4.39 wt %.

The FTIR spectrum of SG (see Figure S2 in the Supporting Information) shows peaks at 1174, 1126, and 1035  $\text{cm}^{-1}$  due to the two S–O bond vibrations and S-phenyl vibration respectively, clearly indicating the presence of  $-\text{SO}_3\text{H}$  group. The peaks at 1011 and 831  $\text{cm}^{-1}$  characterize the C–H in-plane bending and out-of-plane hydrogen wagging vibrations of  $p$ -disubstituted phenyl group.<sup>51</sup> Raman spectroscopy is an useful and nondestructive tool to characterize carbon based materials. Figure S3 in the Supporting Information shows the Raman spectra of reduced graphene oxide (RGO) and

sulfonated graphene (SG). The Raman spectrum of RGO exhibits two prominent peaks at 1307 and 1590  $\text{cm}^{-1}$ , which are assigned to the D band (related to the disorder induced phonon mode of vibrations of  $\text{sp}^3$  carbon atoms) and G band (associated with the first-order scattering of  $E_{2g}$  mode for  $\text{sp}^2$  carbon lattice of graphitic domain) respectively.<sup>54</sup> SG exhibits two peaks at 1313 and 1601  $\text{cm}^{-1}$  because of the D and G bands, respectively. The higher energy shift of G band in SG may be attributed to the anchored aryl sulfonic acid group to the graphene sheets causing a difficulty in the lattice vibration of  $\text{sp}^2$  carbon.<sup>55,56</sup> Thus the Raman spectrum of SG reveals successful attachment of  $-\text{SO}_3\text{H}$  groups onto the graphene surface.

Again we have taken the help of XPS spectroscopy to characterize SG and SGRF nanocomposite system. The survey scan XPS spectra and S2p spectra of SG, SGRF are presented in Figure S4a, b in the Supporting Information, which clearly indicate the presence of anchored  $-\text{SO}_3\text{H}$  group on the graphene surface. The shift to lower binding energy of S2p electron in the SGRF (156.2 eV) from that of SG (157 eV) is suggestive of H-bonding interaction between the S=O group of SG and  $-\text{O}-\text{H}$  group of ribityl chain of riboflavin.

The absorption spectra of GO and SG are shown in Figure S5 where GO shows absorption peak at 244 and 302 nm due to the  $\pi-\pi^*$  and  $n-\pi^*$  transition, respectively. SG shows an absorption peak at 265 nm due to the  $\pi-\pi^*$  transition. The red shift of the  $\pi-\pi^*$  transition of SG from that of GO may be attributed to the easier delocalization of  $\pi$ -electrons of graphene ring for the reduction of GO that occurred in the course of sulfonation reaction and the disappearance of  $n-\pi^*$  transition in SG may be as a result of the decrease in concentration of carboxyl, epoxy and carbonyl groups during reduction in the sulfonation process. RF has four absorption peaks at 223, 267, 372, and 446 nm, respectively (see Figure S6 in the Supporting Information); the 223, 267, 446 nm peaks correspond to the  $\pi-\pi^*$  transition, whereas the 372 nm peak is attributed to the  $\pi-\pi^*$  transition coupled with the  $n-\pi^*$  transition.<sup>57,58</sup>

The PL-spectra of SG and GO at pH 4 are presented in Figure 2a, where SG shows 5.5 times higher PL-intensity than that of GO at pH 4. The PL-spectra of SG at pH 7, pH 9.2 and in water are presented in Figure 2b. In water (Figure 2b inset), SG shows a very weak fluorescence property; this may be attributed to the sulfonic acid moieties of SG, which remains ionized as sulfonate ion<sup>51</sup> ( $-\text{SO}_3^-$ ) facilitating nonradiative electron–hole recombination. Also the remaining carboxylate ion<sup>41</sup> in SG plays a similar role, since after the completion of sulfonation reaction there still exist some carboxylic and hydroxyl groups in SG.<sup>50</sup> This sulfonate and remaining carboxylate groups cause a nonradiative electron–hole ( $e-h$ ) recombination yielding poor PL-property of SG in aqueous medium and it is also true at higher pH (pH 7 and 9.2). But at the acidic condition (pH  $\leq 4$ ) the sulfonate and carboxylate groups remain protonated decreasing the nonradiative  $e-h$  recombination to a major extent. Also during the course of the sulfonation reaction, the epoxide and hydroxyl groups of the basal plane of GO becomes significantly reduced, enhancing the PL property of SG, as they are responsible for the poor emissive property of GO.<sup>36,37</sup> So, the better fluorescence property of SG than that of GO may arise because of the formation of larger number of localized  $\text{sp}^2$  domains facilitating more radiative electron–hole recombination. From Table S1 in the Supporting Information, it is also evident that the quantum yield of SG is the highest over GO at pH 4 and also from those of SG at pH

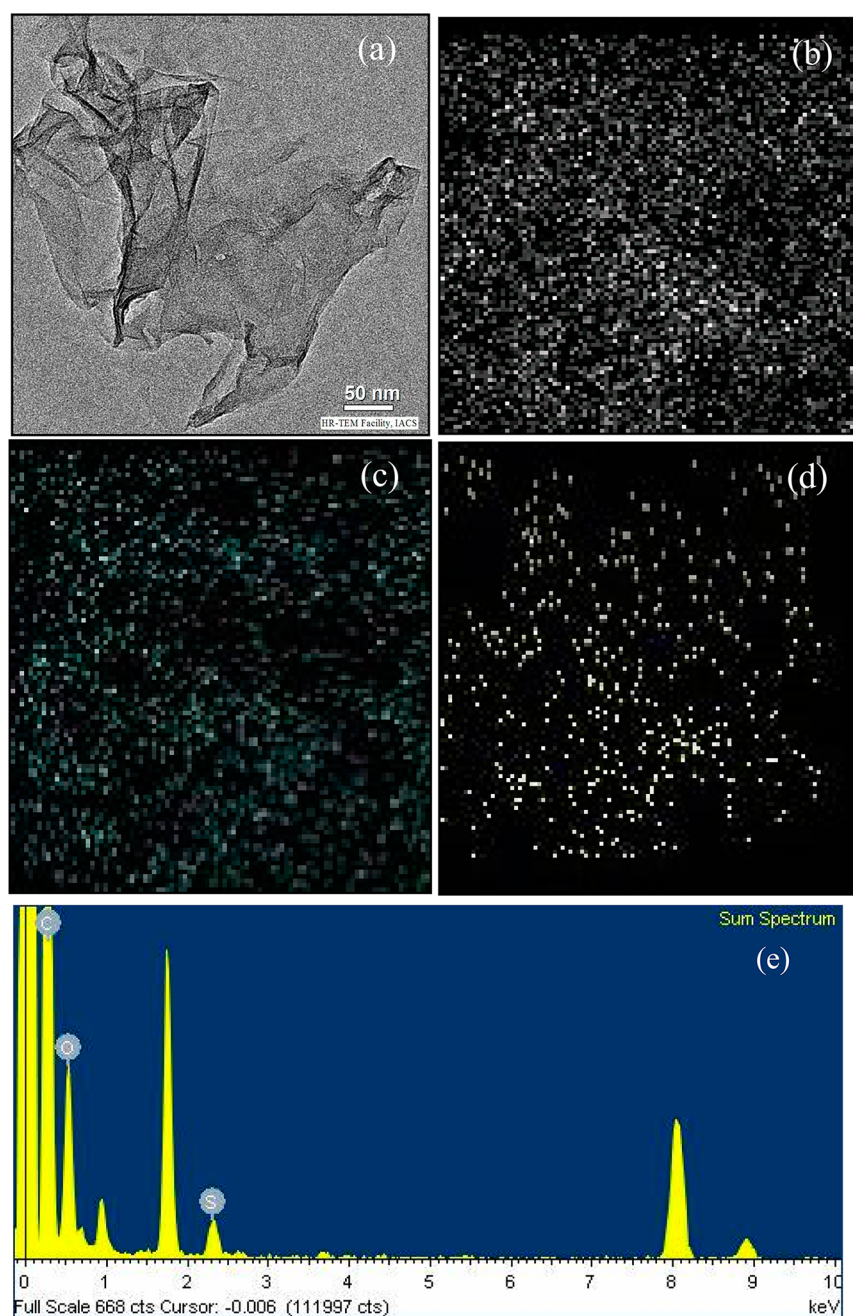


**Figure 1.** TEM image of (a) SG, and corresponding quantitative EDS element mapping of (b) C, (c) O and (d) S and (e) EDS spectrum of SG.

7 and pH 9.2. Also a blue shift of the emission peak at higher pH values is observed in the PL-spectra of SG. This increase in the band gap at higher pH may be due to the ionization of  $-\text{SO}_3\text{H}$ ,  $-\text{COOH}$  and  $-\text{OH}$  groups causing electrostatic doping,<sup>40</sup> which increases the disorderness further. This is evidenced from the pH dependent Raman spectra (see Figure S7 in the Supporting Information) where the D/G intensity ratio of SG increases with increase in pH value (see Table S2 in the Supporting Information).

There are recent reports where GO acts as an acceptor in FRET based system.<sup>59,60</sup> Here, we want to investigate whether GO at pH 4 can act as a donor in the FRET process or not. For this purpose, we have gradually added RF to the GO dispersion and on excitation at 320 nm GO emits at 437 nm (Figure 3). The fluorescence intensity of GO increases even after the

gradual addition of RF with a red shift of 5 nm. So, from the spectrum it is quite evident that GO has not served as a proficient donor, because, if GO may possibly act as a donor the fluorescence intensity of GO after addition of RF should gradually decrease with a blue shift. Though there is a good overlap between the emission spectrum of GO and absorption spectrum of RF (Figure 4a) the low quantum yield of GO at pH 4 (see Table S1 in the Supporting Information) is the possible reason for not acting as a donor. It is to be noted here that the emission peak at 521 nm is due to RF, which increases because of the increased concentration of the chromophore.

The integral overlap spectrum of SG and RF has been presented in Figure 4b. This spectrum noticeably indicates a strong overlap between the emission spectrum of SG and absorption spectrum of RF and we hope an efficient FRET

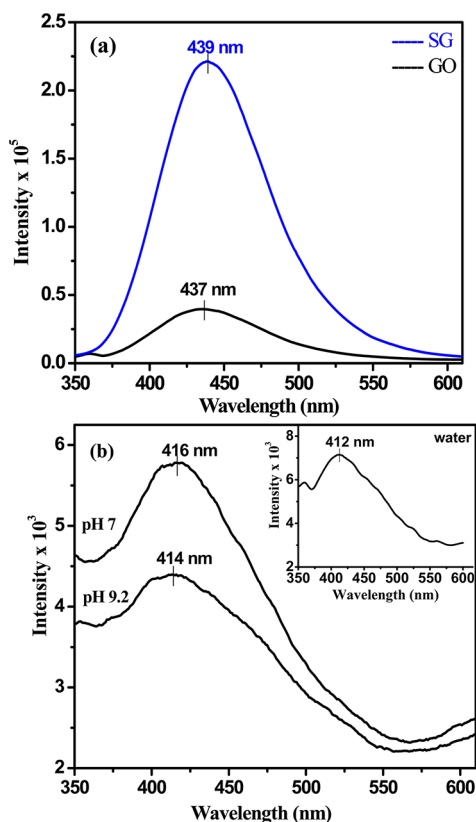


**Figure 2.** Fluorescence spectra of (a) SG, GO at pH 4 and (b) that of SG at pH 7, pH 9.2, and in water (inset).

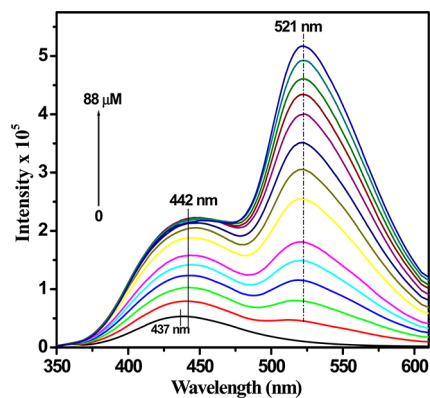


**Figure 3.** Fluorescence emission spectra of GO upon gradual addition of RF for excitation at 320 nm.

process from SG (donor) to RF (acceptor) as the quantum yield of SG is  $\sim 6$  times higher than that of GO. The emission spectrum of SG with various concentrations of RF has been depicted in Figure 5 and it is evident that the fluorescence intensity of SG decreases regularly with increasing concentration of RF. A new fluorescence peak at 527 nm is observed for RF, with a clear isoemissive point at 489 nm. The spectra also indicate that the addition of RF to SG leads to a significant blue shift in the emission wavelength of SG from 439 to 426 nm with a considerable quenching of fluorescence emission of SG indicating the FRET process to occur in the system. This is in sharp contrast to the GO/RF system discussed above and here the emission peak of RF also shows a red shift of 6 nm (Figure 3), indicating better delocalization of  $\pi$ -electrons of RF in the SG/RF system. Probably because of the strong

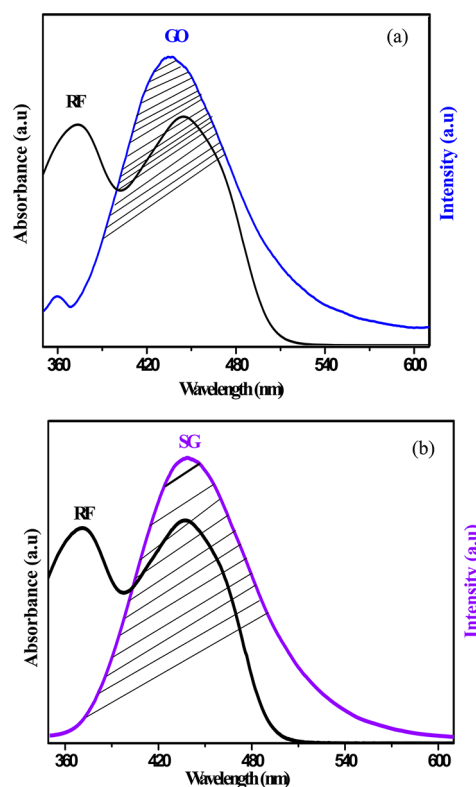


**Figure 4.** Integral overlap between emission spectrum of (a) GO and absorption spectrum of RF and (b) SG and absorption spectrum of RF.

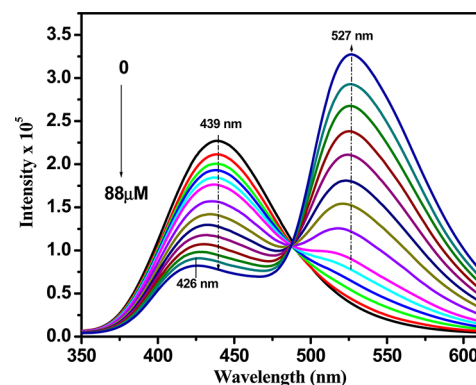


**Figure 5.** Fluorescence spectra of SG (0.004% w/v) with various concentrations of RF for excitation at 320 nm.

interaction between SG and RF they come closer to each other which causes better delocalization of  $\pi$ -electrons of RF. A comparison of fluorescence intensity of RF in RF/GO and in RF/SG systems indicate that the PL intensity of RF is lower in the latter case, suggesting some quenching and closer proximity between SG and RF compared to the other pair is the probable cause. The efficiency of energy transfer process has been determined from the steady-state measurement using the following equation<sup>2,5</sup>

$$E = 1 - I_{DA}/I_D \quad (2)$$

where  $I$  is the relative donor fluorescence intensity in the absence ( $I_D$ ) and presence ( $I_{DA}$ ) of the acceptor (see Table S3 in the Supporting Information). For 4  $\mu\text{M}$  addition of RF only 7% energy transfer takes place, whereas for 88  $\mu\text{M}$  addition of

RF to SG it is almost 64%, so with gradual addition of RF the energy transfer efficiency increases.

Again to get a better insight of the FRET phenomenon, we have calculated the Förster distance using the following equation<sup>5</sup>

$$R_0^6 = \frac{9000(\ln 10)\kappa^2\phi_D}{128\pi^5Nn^4}J(\lambda) \quad (3)$$

where  $\phi_D$  is the quantum yield of the donor in absence of acceptor,  $N$  is Avogadro's number,  $n$  is the refractive index of the medium,  $J(\lambda)$  is the spectral overlap integral, which expresses the degree of spectral overlap between the donor emission and the acceptor absorption. The spectral overlap integral is defined as the following

$$J(\lambda) = \int_0^\infty F_D(\lambda)\varepsilon_A(\lambda)\lambda^4d\lambda \quad (4)$$

where  $F_D(\lambda)$  is the normalized emission spectrum of donor and it is dimensionless,  $\varepsilon_A(\lambda)$  is the absorption coefficient of acceptor, and  $\kappa^2$  is the orientation factor, which describes the relative orientation of the transition dipoles of the donor and acceptor in space. The value of  $\kappa^2$  is usually assumed to be 2/3, which is appropriate for randomly oriented dipoles of donor and acceptor. If  $\varepsilon_A(\lambda)$  is expressed in units of  $M^{-1} \text{ cm}^{-1}$  and  $\lambda$  is in nanometers, then  $J(\lambda)$  is in units of  $M^{-1} \text{ cm}^{-1} \text{ nm}^4$ . In our donor–acceptor-based system the spectral overlap integral is calculated to be  $1.77 \times 10^{13} M^{-1} \text{ cm}^{-1} \text{ nm}^4$ . The estimated value of Förster distance in our donor–acceptor based pair is found to be 2.61 nm, which is much below the maximum distance ( $\sim 10$  nm) between the donor and acceptor required for the FRET process indicating efficient energy transfer between donor–acceptor pair.<sup>5</sup>

Here, we have employed the FRET process to detect vitamin B<sub>2</sub> (RF), in presence of nucleic acids (DNA, RNA), amino acid (lysine), protein (BSA). The FRET process of SG/RF system is occurring in the presence of these biological samples. With the addition of DNA, RNA (Figure 6a, b) and BSA, lysine (see Figure S8a, b in the Supporting Information) fluorescence intensity of SG increases at first to some extent but upon gradual addition of RF to the system the energy transfer process starts showing a gradual decrease of fluorescence intensity of SG. The small initial increase in fluorescence intensity in all cases may be due to the certain degree of passivation of SG surface with the biological molecules decreasing the nonradiative recombination of electron–hole pair. Further we have tried to detect RF from the pharmaceutical samples like Becosules and Zevit (see Figure S9a, b in the Supporting Information). It is obvious from the spectra that inspite of the presence of different water-soluble vitamins and other components in Becosules and Zevit (see Table S4 in the Supporting Information) the fluorescence energy transfer process is persistent. So, SG can be very conveniently used as a simple platform to detect vitamin B<sub>2</sub> in presence of biomolecules as well as other water-soluble vitamins. We have tried to determine vitamin B<sub>2</sub> in the presence of blood serum, though we are unable to determine the amount of vitamin B<sub>2</sub> in the blood serum directly because of the very low level (0.11  $\mu\text{g}/\text{mL}$ ) of vitamin B<sub>2</sub> in blood serum.<sup>61</sup> But from the spectrum of Figure S10 in the Supporting Information, it is evident that energy transfer process is occurring in presence of blood serum, so we can determine vitamin B<sub>2</sub> in the presence of blood serum by the

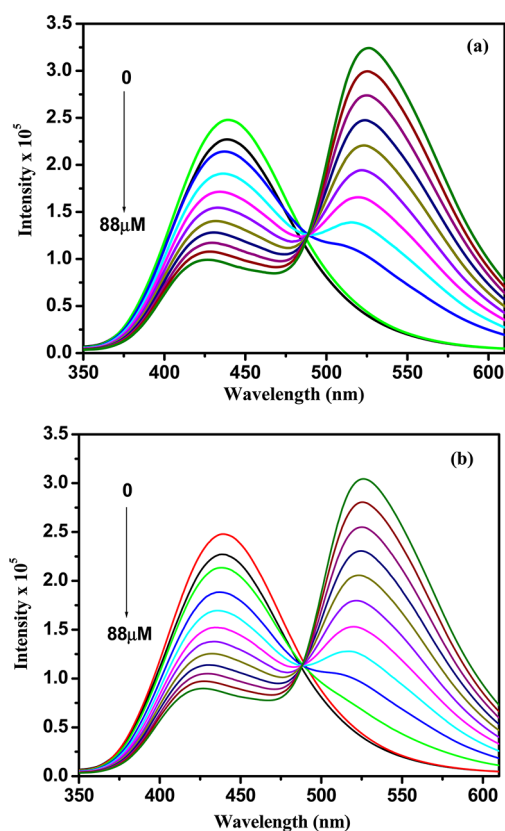


**Figure 6.** Fluorescence spectra of SG (0.004% w/v) with various concentrations of RF in the presence of (a) DNA and (b) RNA for excitation at 320 nm.

FRET method. Basically there is no difference between the FRET efficiencies in presence of different biomolecules as evident from the almost same fluorescence intensity values of SG/RF system in presence of DNA, RNA, BSA, Lysine and blood serum (cf. Figure 6a, b; Figure S8a, b and S10 in the Supporting Information). We have aimed to check whether FRET process is persistent in presence of biomolecules or not, and there is no change of FRET efficiency of SGRF system (Figure 5) in the presence of biomolecules. That is the reason for choosing the FRET process to detect RF in the presence of biomolecules.

The calibration curve for the detection of RF has been presented in Figure S11 in the Supporting Information, where  $I_0$  is the fluorescence intensity of donor (SG) in absence of the acceptor (RF) and  $I$  is that in the presence of acceptor RF. The calibration plot shows excellent promise to detect RF quantitatively, because if we know the relative fluorescence intensity ( $I_0/I$ ) of any RF-containing sample, it is very easy to get the amount of RF present in the sample from the calibration plot. From the calibration curve, the limit of detection (LOD) of vitamin B<sub>2</sub> in our method has been calculated using the formula  $\text{LOD} = 3 \times (\text{SD})_{\text{Blank}}/S$ , where SD is the standard deviation of background fluorescence, i.e., in the absence of acceptor (RF) and  $S$  is the slope of the calibration curve. The LOD of vitamin B<sub>2</sub> to get a signal in our system is calculated to be 0.6  $\mu\text{g}/\text{mL}$  from calibration curve (see Figure S11 in the Supporting Information), which is close to the concentration detected by HPLC method (0.2–0.4  $\mu\text{g}/\text{mL}$ ).<sup>62–64</sup> It indicates that the HPLC method is somewhat superior to the present FRET method, but complexity in the

former method may arise in presence of biomolecules. Also considering the costly solvents used in HPLC, the present FRET is a cost-effective, less time-consuming and easier operative method that would make it attractive for efficient detection of RF in presence of other biomolecules.

To check the selectivity of our system, we have performed another experiment using structurally similar biomolecule like RF namely Flavin mononucleotide (FMN). Fluorescence spectra of SG with various concentrations of FMN are exhibited in Figure S12 in the Supporting Information, which clearly specify that similar FRET process is occurring as that of RF. So, in general, we can infer that SG can be used as a donor to detect biomolecule containing Flavin moiety.

We have also performed blank fluorescence experiments using RF, Zevit, and Becosule (see Figure S13a–c in the Supporting Information) to check the superiority of FRET method over the direct fluorescence method. The spectra clearly indicate that direct method of determining RF from Zevit and Becosule leads to lower fluorescence intensity than that of the blank experiment using pure RF. This erroneous result is due to the presence of different components in the capsule causing quenching of the fluorescence intensity. The calibration curve for blank experiment is shown in Figure S14 in the Supporting Information. The determination of RF by FRET and classical fluorescence method has been compared from the above two calibration curves (see Figures S11 and S14 in the Supporting Information) for Zevit and Becosule and is presented in Table S5 in the Supporting Information. These results clearly indicate that the classical fluorescence method produces a significantly erroneous result in the determination of RF in Zevit and Becosule, rather our present FRET experiment produces the results which match to the values certified by the drug companies. So the present method based on the FRET process describes a simple approach to detect RF/flavin moiety in the presence of different biomolecules involving SG as a donor and it is superior to the ordinary fluorescence method of detecting RF.

## CONCLUSION

The present work demonstrates a facile approach to prepare fluorescent sulfonated graphene (SG) which has been used to detect vitamin B<sub>2</sub>. Upon photoexcitation at 320 nm, we have observed efficient energy transfer from SG (donor) to RF (acceptor) and utilized the spontaneous FRET phenomenon to detect vitamin B<sub>2</sub> in the presence of biomolecules like DNA, RNA, lysine, BSA, blood serum, and other water-soluble commercial vitamin capsules. To the best of our knowledge, we report here the detection of vitamin B<sub>2</sub> in aqueous medium using the FRET property of a graphene derivative for the first time. The fluorescent sulfonated graphene can be further used for various purposes like preparation of new fluorescent graphene composites, which will pave a new way in developing different efficient chemical and biochemical sensors.

## ASSOCIATED CONTENT

### Supporting Information

Tables of quantum yield values of SG; D/G intensity ratio of SG at different pH and FRET efficiency of SG-RF pair; TEM image and EDS elemental mapping of GO; FTIR spectrum of SG; Raman spectra of RGO and SG; XPS spectra of SG and SGRF; UV–vis spectrum of GO, SG and RF; PL-spectra of different systems; table of composition of Zevit and Becosule capsules; calibration curve of SG-RF and blank; table for

determination of RF, etc. This material is available free of charge via the Internet at <http://pubs.acs.org/>.

## AUTHOR INFORMATION

### Corresponding Author

\*E-mail: [psuakn@iacs.res.in](mailto:psuakn@iacs.res.in). Fax: (+91) 33 2473 2805.

### Notes

The authors declare no competing financial interest.

## ACKNOWLEDGMENTS

We gratefully acknowledge CSIR (Grant 02(0051)/12/EMR-II) New Delhi and DST Unit of Nanoscience at IACS for financial support. A.K. and S.N. gratefully acknowledge CSIR, New Delhi for granting the fellowship. We acknowledge Dr. N. R. Jana and A. Saha of IACS for helping in micro Raman spectroscopy. We also acknowledge Sadananda Mandal of IACS for his assistance in calculating Förster distance.

## REFERENCES

- (1) Andrews, D. L.; Bradshaw, D. S. *Encyclopedia of Applied Physics*; Wiley Online Library: New York, 2009; pp 533–554.
- (2) Sapsford, K. E.; Berti, L.; Medintz, I. L. *Angew. Chem., Int. Ed.* **2006**, *45*, 4562–4589.
- (3) Jockers, R.; Marullo, S. *Encyclopedia of Genetics, Genomics, Proteomics and Bioinformatics*; Wiley Online Library: New York, 2005.
- (4) Huang, X. Y.; Li, L.; Qian, H. F.; Dong, C. Q.; Ren, J. *Angew. Chem., Int. Ed.* **2006**, *45*, 5140–5143.
- (5) Lakowicz, J. R. *Principles of Fluorescence Spectroscopy*, 3rd ed.; Springer: New York, 2006; p 443–460.
- (6) Arkin, M. R.; Stemp, E. D. A.; Turro, C.; Turro, N. J.; Barton, J. K. *J. Am. Chem. Soc.* **1996**, *118*, 2267–2274.
- (7) He, F.; Tang, Y. L.; Wang, S.; Li, Y. L.; Zhu, D. B. *J. Am. Chem. Soc.* **2005**, *127*, 12343–12346.
- (8) Dongen, E. M. W. M. V.; Dekkers, L. M.; Spijker, K.; Meijer, E. W.; Klomp, L. W. J.; Merckx, M. *J. Am. Chem. Soc.* **2006**, *128*, 10754–10762.
- (9) Hink, M. A.; Visser, N. V.; Borst, J. W.; Hoek, A. V.; Visser, A. J. W. G. *J. Fluoresc.* **2003**, *13*, 185–188.
- (10) Zhang, X. L.; Xiao, Y.; Qian, X. H. *Angew. Chem., Int. Ed.* **2008**, *47*, 8025–8029.
- (11) Albers, A. E.; Okreglak, V. S.; Chang, C. J. *J. Am. Chem. Soc.* **2006**, *128*, 9640–9641.
- (12) Zhou, Z. G.; Yu, M. X.; Yang, H.; Huang, K. W.; Li, F. Y.; Yi, T.; Huang, C. H. *Chem. Commun. (Cambridge, U. K.)* **2008**, 3387–3389.
- (13) Chen, L.; Lee, S.; Lee, M.; Lim, C.; Choo, J.; Park, J. Y.; Lee, S.; Joo, S. W.; Lee, K. H.; Choi, Y. W. *Biosens. Bioelectron.* **2008**, *23*, 1878–1882.
- (14) Foraker, A. B.; Khantwal, C. M.; Swaan, P. W. *Adv. Drug Delivery Rev.* **2003**, *55*, 1467–1483.
- (15) Gastaldi, G.; Ferrari, G.; Verri, A.; Casirola, D.; Orsenigo, M. N.; Laforenza, U. *J. Nutr.* **2000**, *130*, 2556–2561.
- (16) Batey, D. W.; Eckhart, C. D. *Anal. Biochem.* **1990**, *188*, 164–167.
- (17) Cristina, A. L.; Fulvio, M.; Deigo, T. J. *Chromatogr. A* **1998**, *823*, 355–363.
- (18) Tang, X.; Cronin, D. A.; Brunton, N. P. *J. Food Compos. Anal.* **2006**, *19*, 831–837.
- (19) Hu, L.; Yang, X.; Wang, C.; Yuan, H.; Xiao, D. *J. Chromatogr. B* **2007**, *856*, 245–251.
- (20) Cataldi, T. R. I.; Donatella, N.; Giuseppe, E. D. B.; Sabino, A. B. *J. Chromatogr. A* **2002**, *968*, 229–239.
- (21) Dikin, D. A.; Stankovich, S.; Zimney, E. J.; Piner, R. A.; Dommett, G. H. B.; Evmenenko, G.; Nguyen, S. T.; Ruoff, R. S. *Nature* **2007**, *448*, 457–460.
- (22) Yang, W.; Ratinac, K. R.; Ringer, S. P.; Thordarson, P.; Gooding, J. J.; Braet, F. *Angew. Chem., Int. Ed.* **2010**, *49*, 2114–2138.

- (23) Cai, W. W.; Piner, R. D.; Stadermann, F. J.; Park, S.; Shaibat, M. A.; Ishii, Y. *Science* **2008**, *321*, 1815–1817.
- (24) Dai, L.; He, P. G.; Li, S. N. *Nanotechnology* **2003**, *14*, 1081–1097.
- (25) Mohanty, N.; Berry, V. *Nano Lett.* **2008**, *8*, 4469–4476.
- (26) Zuo, X.; He, S.; Li, D.; Peng, C.; Huang, Q.; Song, S.; Fan, C. *Langmuir* **2010**, *26*, 1936–1939.
- (27) Sun, X.; Liu, Z.; Welsher, K.; Robinson, J. T.; Goodwin, A.; Zaric, S.; Dai, H. *Nano Res.* **2008**, *1*, 203–212.
- (28) Lu, C. H.; Yang, H. H.; Zhu, C. L.; Chen, X.; Chen, G. N. *Angew. Chem., Int. Ed.* **2009**, *48*, 4785–4787.
- (29) Dong, H.; Gao, W.; Yan, F.; Ji, H.; Ju, H. *Anal. Chem.* **2010**, *82*, 5511–5517.
- (30) Zhang, M.; Yin, B. C.; Tan, W.; Ye, B. C. *Biosens. Bioelectron.* **2011**, *26*, 3260–3265.
- (31) Descalzo, A. B.; Manez, R. M.; Sancenon, F.; Hoffmann, K. *Angew. Chem., Int. Ed.* **2006**, *45*, 5924–5948.
- (32) Heller, D. A.; Jeng, E. S.; Yeung, T. K.; Martinez, B. M.; Moll, A. E.; Gastala, J. B.; Strano, M. S. *Science* **2006**, *311*, 508–511.
- (33) Liu, Y.; Yu, D.; Zeng, C.; Miao, Z.; Dai, L. *Langmuir* **2010**, *26*, 6158–6160.
- (34) Guo, S.; Dong, S. *Chem. Soc. Rev.* **2011**, *40*, 2644–2672.
- (35) Wen, Y.; Xing, F.; He, S.; Song, S.; Wang, L.; Long, Y.; Li, D.; Fan, C. *Chem. Commun. (Cambridge, U. K.)* **2010**, *46*, 2596–2598.
- (36) Mei, Q.; Zhang, K.; Guan, G.; Liu, B.; Wang, S.; Zhang, Z. *Chem. Commun. (Cambridge, U. K.)* **2010**, *46*, 7319–7321.
- (37) Subrahmanyam, K. S.; Kumar, P.; Nag, A.; Rao, C. N. R. *Solid State Commun.* **2010**, *150*, 1774–1777.
- (38) Eda, G.; Lin, Y.; Mattevi, C.; Yamaguchi, H.; Chen, H.; Chen, L.; Chen, C.; Chhowalla, M. *Adv. Mater. (Weinheim, Ger.)* **2010**, *22*, 505–509.
- (39) Loh, K. P.; Bao, Q.; Eda, G.; Chhowalla, M. *Nature chemistry* **2010**, *2*, 1015–1024.
- (40) Zhao, W.; Song, C.; Pehrsson, P. E. *J. Am. Chem. Soc.* **2002**, *124*, 12418–12419.
- (41) Chen, J. L.; Yan, X. P. *Chem. Commun. (Cambridge, U. K.)* **2011**, *47*, 3135–3137.
- (42) Galande, C.; Mohite, A. D.; Naumov, A. V.; Gao, W.; Ci, L.; Ajayan, A.; Gao, H.; Srivastava, A.; Weisman, R. B.; Ajayan, P. M. *Sci. Rep.* **2011**, *1*, 85, 1–5.
- (43) Shang, J.; Ma, L.; Li, J.; Ai, W.; Yu, T.; Gurzadyan, G. G. *Sci. Rep.* **2012**, *2*, 792, 1–8.
- (44) Chen, J. L.; Yan, X. P.; Meng, K.; Wang, S. F. *Anal. Chem.* **2011**, *83*, 8787–8793.
- (45) Kundu, A.; Layek, R. K.; Nandi, A. K. *J. Mater. Chem.* **2012**, *22*, 8139–8144.
- (46) Kundu, A.; Layek, R. K.; Kuila, A.; Nandi, A. K. *ACS Appl. Mater. Interfaces* **2012**, *4*, 5576–5582.
- (47) Fu, X.; Chen, L.; Li, J.; Lin, M.; You, H.; Wang, W. *Biosens. Bioelectron.* **2012**, *34*, 227–231.
- (48) Ji, J.; Zhang, G.; Chen, H.; Wang, S.; Zhang, G.; Zhang, F.; Fan, X. *Chem. Sci.* **2011**, *2*, 484–487.
- (49) Zhao, G.; Jiang, L.; He, Y.; Li, J.; Dong, H.; Wang, X.; Hu, W. *Adv. Mater. (Weinheim, Ger.)* **2011**, *23*, 3959–3963.
- (50) Nandi, S.; Routh, P.; Layek, R. K.; Nandi, A. K. *Biomacromolecules* **2012**, *13*, 3181–3188.
- (51) Si, Y.; Samulski, E. T. *Nano Lett.* **2008**, *8*, 1679–1682.
- (52) Szabo, T.; Berkesi, O.; Forgo, P.; Josepovits, K.; Sanakis, Y.; Petridis, D. *Chem. Mater.* **2006**, *18*, 2740–2749.
- (53) Hummers, W. S.; Offeman, R. E. *J. Am. Chem. Soc.* **1958**, *80*, 1339.
- (54) Ferrari, A. C.; Meyer, J. C.; Scardaci, V.; Casiraghi, C.; Lazzeri, M.; Mauri, F.; Piscanec, S.; Jiang, D.; Novoselov, K. S.; Roth, S.; Geim, A. K. *Phys. Rev. Lett.* **2006**, *97*, 187401 (1–4)..
- (55) Kudin, K. N.; Ozbas, B.; Schniepp, H. C.; Prud'homme, R. K.; Aksay, I. A.; Car, R. *Nano Lett.* **2008**, *8*, 36–41.
- (56) Lazzeri, M.; Mauri, F. *Phys. Rev. Lett.* **2006**, *97*, 266407 (1–4)..
- (57) Heelis, P. F. *Chem. Soc. Rev.* **1982**, *11*, 15–39.
- (58) Manna, S.; Saha, A.; Nandi, A. K. *Chem. Commun. (Cambridge, U. K.)* **2006**, 4285–4287.
- (59) Zhang, C.; Yuan, Y.; Zhang, S.; Wang, Y.; Liu, Z. *Angew. Chem.* **2011**, *123*, 6983–6986.
- (60) Piao, Y.; Liu, F.; Seo, T. S. *Chem. Commun. (Cambridge, U. K.)* **2011**, *47*, 12149–12151.
- (61) Rokitzki, L.; Sagredos, A.; Keck, E.; Saver, B.; Keul, J. *J. Nutr. Sci. Vitaminol.* **1994**, *40*, 11–22.
- (62) Hassan, O.; Chee, M. J. *Malaysian J. Anal. Sci.* **2001**, *7*, 251–255.
- (63) Ekinci, R.; Kadakal, Ç. *Acta Chromatogr.* **2005**, *15*, 289–297.
- (64) Thomas, S.; Sharma, A.; Issarani, R.; Nagori, B. P. *Indian J. Chem. Technol.* **2008**, *15*, 598–603.